

Research Article

Efficient Photoluminescence of Mn^{2+} -Doped ZnS Quantum Dots Sensitized by Hypocrellin A

Xianlan Chen,^{1,2} Wei Liu,^{1,2} Guowei Zhang,^{1,2} Na Wu,^{1,2} Ling Shi,^{1,2} and Shanqing Pan^{1,2}

¹School of Science, Honghe University, Mengzi, Yunnan 661100, China

²Key Laboratory of Natural Pharmaceutical & Chemical Biology of Yunnan Province, Mengzi, Yunnan 661100, China

Correspondence should be addressed to Wei Liu; liuwei4728@126.com

Received 19 December 2014; Revised 25 March 2015; Accepted 22 April 2015

Academic Editor: Sule Erten-Ela

Copyright © 2015 Xianlan Chen et al. This is an open access article distributed under the Creative Commons Attribution License, which permits unrestricted use, distribution, and reproduction in any medium, provided the original work is properly cited.

Mn^{2+} -doped ZnS semiconductor quantum dots reveal remarkably intense photoluminescence with the $^4T_1(4G) \rightarrow ^6A_1(6S)$ transition. In this study, following growth doping technique, Mn^{2+} -doped ZnS quantum dots (ZnS: Mn^{2+} QDs) with high-quality optical properties and narrow size distribution were synthesized successfully. The dopant emission has been optimized with various reaction parameters, and it has been found that the percentage of introduced dopant, reaction temperature, and time as well as the pH of a reaction mixture are key factors for controlling the intensity. Photoluminescence emission (PL) measurements of ZnS: Mn^{2+} QDs show Mn^{2+} d-d orange luminescence along with band-edge blue luminescence. Moreover, the electron transfer from singlet states of hypocrellin A (HA) to colloidal ZnS: Mn^{2+} QDs has been examined by absorption spectra and fluorescence quenching. The absorption spectrum gave an evidence of the increases in the extinction coefficient and the red-shift of the absorption maxima in the absorption spectra of HA in the presence of ZnS: Mn^{2+} QDs, demonstrating the occurrence of surface interactions between the sensitizer and the particle surface. Fluorescence quenching by ZnS: Mn^{2+} QDs also suggested that there were a complex association between HA and ZnS: Mn^{2+} QDs, which was necessary for observing the heterogeneous electron-transfer process at the interface of sensitizer-semiconductor.

1. Introduction

Light emitting semiconductor nanocrystals, otherwise known as quantum dots (QDs), have been widely investigated during the last two decades in view of their size-tunable optical properties, wide range of excitations, emission color purity, high quantum efficiency, and applications as a light emitting source in various optoelectrical devices, imaging, solar cells, environment, remediation, and therapeutics and in biological applications [1, 2]. Unfortunately, QDs, now in general use in many fields, have been so far composed of toxic compounds (Cd, Pb, Hg, Te, As, etc.) [3]. The main advantages of Mn-doped ZnS dots compared to Cd-based QDs are their lower cytotoxicity, higher excited state lifetimes, and enhanced thermal and environmental stability [4]. Interestingly, control over size and shape, doping with impurities, and functionalization with organic or biological moieties have been the primary strategies for control over optical and electrical properties, especially the emission properties of the quantum

dots [5]. In recent developments, high-quality doped semiconductor nanocrystals are being explored as viable alternatives to undoped nanocrystals with additional advantages such as larger Stokes shift to avoid self-absorption, enhanced thermal and environmental stabilities, and minimized toxicity [6].

ZnS is the most studied II-VI compound with band gap energy of 3.6 eV and has sufficiently intrigued an enormous amount of researchers to devote themselves to researching in this hot field for its excellent properties [7]. The doping of ZnS semiconductor nanocrystals by the incorporation of atomic impurities is routinely used to modify their electrical and optical properties [8, 9]. A demonstrated ability to introduce transition-metal impurities into semiconductor quantum dots and, hence, to form doped nanostructures has indeed opened up a new branch in the field of nanoscience [10–12]. The luminescence of Mn^{2+} -doped II-VI semiconductor quantum dots due to the $^4T_1(4G) \rightarrow ^6A_1(6S)$ transition is much higher than that of their bulk counterpart [13]. Recently,

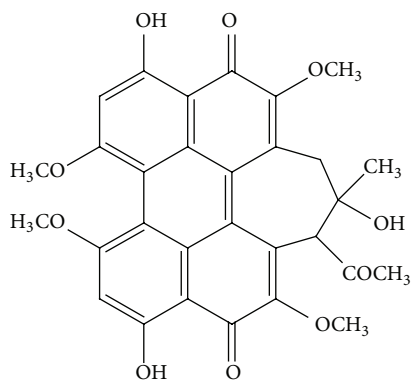


FIGURE 1: Chemical structures of hypocrellin A.

many groups have reported a variety of methods to synthesize Mn^{2+} -doped ZnS with different nanostructures, such as nanorods, nanowires (NWs), and nanotubes, which have been widely studied because of their unique physicochemical characteristics and numerous applications in mesoscopic physics and the fabrication of nanodevices [14–16]. Moreover, Mn^{2+} is an ideal dopant, as it can provide luminescent center and can also reveal hyperfine splitting in electron paramagnetic resonance spectra [17]. The Mn^{2+} dopant functions as emissive traps because the trap energy levels lie between the valence and conduction bands of the host crystal [18]. The trap states thus change the optical and electronic properties of the host. It is widely believed that the excitation takes place through the host lattice and is followed by energy transfer to the impurity to yield the Mn luminescence band in Mn^{2+} -doped ZnS quantum dots.

The photosensitization of a stable, large-band gap semiconductor ZnS by organic dyes is an interesting and useful phenomenon that was used to extend its absorptive range [19]. Hypocrellin A (HA) is a new type of photosensitizer (Figure 1), isolated from the fungus *Hypocrella bambuse*. Recently, the chemistry, photochemistry, and photophysics of HA have been studied and reviewed [20], but photosensitization of the doping semiconductor nanocrystals with HA by the injection of electrons from its singlet excited state in aqueous solution is little studied. In the present study, we report here large-scale synthesis of high-quality Mn^{2+} -doped ZnS nanocrystals using common and inexpensive chemicals following a simple and reproducible synthetic technique; HA acting as an electron donor adsorbs directly onto the surface of Mn^{2+} -doped ZnS nanocrystals and can transfer an electron from its singlet excited state into the conduction band of Mn^{2+} -doped ZnS nanocrystals.

2. Experimental

2.1. Reagents and Apparatus

2.1.1. Reagents. ZnSO_4 , L-cysteine, sodium sulfide (55–58%), manganese acetate tetrahydrate (99%), and NaOH were analytical grade reagents. All chemicals were purchased from

Aldrich. In the reaction solution, the Mn concentration was varied (by varying the $\text{Mn}(\text{CH}_3\text{COO})_2 \cdot 4\text{H}_2\text{O}$ amount in the organometallic precursor) to values of 0.0%, 1.0%, 2.0%, 3.0%, 4.0%, and 5.0%.

2.1.2. Apparatus. The UV-visible spectra (Perkin-Elmer Lambda 900 USA) and photoluminescence (PL) emission spectra were recorded in a Hitachi F-7000 fluorescence photometer. All measurements were conducted at room temperature.

2.2. Synthesis of ZnS Nanoparticles. For the synthesis of ZnS QDs, we have employed a simple aqueous method using zinc sulfate, sodium sulfide, and manganese acetate tetrahydrate as the starting materials. The L-cysteine was used as the complexing agent and Milli-Q grade water as the solvent. First, 50 mL 0.03 M L-cysteine and 5 mL 0.1 M ZnSO_4 solutions were placed in three-necked flask equipped with magnetic stirring bars. Second, a certain amount of NaOH solutions was slowly dropped into flask to make pH of the reaction mixture to 11.5 through a syringe controlled by a step motor. Then, N_2 was introduced to rule out oxygen in solution for 30 min while thoroughly stirring. Finally, 5 mL 0.1 M Na_2S was rapidly dropped into the mixtures through a syringe. After the addition of Na_2S , the final solutions were stirred for another 4.5 h under totally enclosed condition at ambient temperature. The ZnS QDs were collected by centrifuging at 4,000 rpm for 20 min and washed 2–3 times with Milli-Q water.

2.3. Synthesis of Mn^{2+} -Doped ZnS ($\text{ZnS}:\text{Mn}^{2+}$) Nanoparticles. A main objective of our research in this area of $\text{ZnS}:\text{Mn}^{2+}$ quantum dots is to investigate the optimal conditions for their synthesis in the aqueous medium from readily available precursors. The dopant emission has been optimized with varying reaction parameters, and it has been found that the pH of an aqueous solution, the reaction temperature, and reaction time as well as the percentage of introduced dopant in the reaction mixture are key factors for controlling the intensity. A second objective of our program is to investigate photochemical events during the photosensitization of hypocrellin A on highly luminescent Mn^{2+} -doped ZnS nanocrystals.

The $\text{ZnS}:\text{Mn}^{2+}$ QDs were synthesized by the following general procedure. 50 milliliters of an aqueous solution of L-cysteine (0.03 M) was added to 5 mL of ZnSO_4 (0.1 M) under vigorous stirring. Then a certain amount of $\text{Mn}(\text{CH}_3\text{COO})_2$ and $4\text{H}_2\text{O}$ (0.2 M) was added to this solution, and a certain amount of NaOH solutions was slowly dropped to adjust to the pH value of the mixtures. Interestingly, L-cysteine can resolve to $^-\text{SCH}_2\text{CH}(\text{NH}_2)\text{COO}^-$ complexation with Zn^{2+} and Mn^{2+} easily in alkaline condition, which is apt to prepare $\text{ZnS}:\text{Mn}^{2+}$ QDs. N_2 was introduced to rule out oxygen into solution for 30 min while thoroughly stirring. Next, 5 mL of Na_2S (0.5 M) was rapidly dropped into the mixtures through a syringe. The reaction temperature was maintained at various certain temperatures (30°C, 40°C, 50°C, 60°C, and 70°C) for a certain period of time (3 h, 3.5 h, 4 h, 4.5 h, 5 h, and 5.5 h) under constant stirring in totally enclosed condition. Finally,

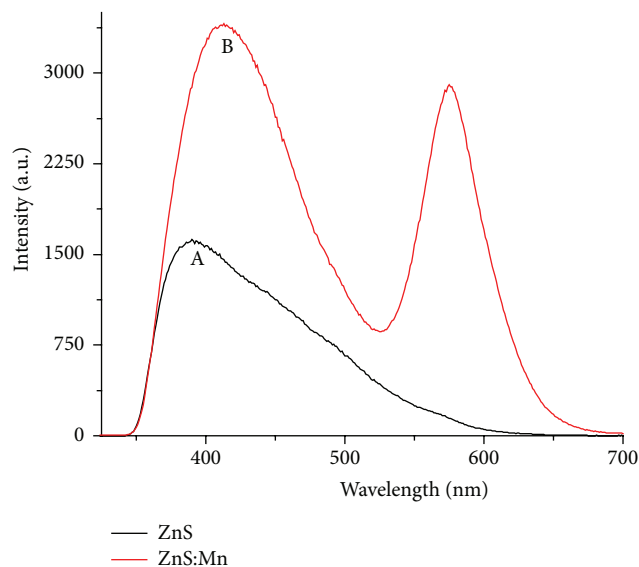


FIGURE 2: Fluorescence emission spectra of ZnS and ZnS:Mn²⁺ QDs. The excitation wavelength for all the samples was fixed at 300 nm.

the ZnS:Mn²⁺ QDs were isolated by centrifugation, washed three times with Milli-Q water and then with cold ethanol (95% v/v), dried under vacuum for 24 h, and ground in an agate mortar.

2.4. Preparation of Hypocrellin A (HA). HA was extracted and purified according to the method described by Brockman and Spitzner [21]. Firstly, 10 g *Hypocrella bambuase* was wrapped by filter paper and put into Soxhlet extractor. 50 mL acetone was placed in the round bottom flask, and the reaction mixture was allowed to stir for 10 h under refluxing condition and extracted repeatedly HA until extract became light in color. In the second step, the extracting solution was moved to Rotary evaporators and condensed into a sanguineous concentrated solution by vacuum distillation. The crystallization precipitation of HA was collected under natural cooling and then was dissolved in 10% NaOH and washed with petroleum ether repeatedly. HCl was used to neutralize excess NaOH, and then the extracts were extracted with trichloromethane repeatedly. Finally, the crude extract of HA was purified and separated by silicon thin layer chromatography, petroleum ether, and ethyl acetate, and 95% alcohol was blended with 4 : 2 : 1 (v/v) and used as developing solvent.

3. Results and Discussion

3.1. UV-Visible Absorption and Photoluminescence Characteristics of the ZnS:Mn²⁺ QDs. Doping introduces new levels within the band gap, modifying the linear photophysical properties of ZnS QDs, particularly the photoluminescence of ZnS QDs. Room-temperature photoluminescence emission (PL) spectra in Mn²⁺-doped ZnS QDs (Figure 2(B)) show emission peaking around 585 nm, attributed to the transition from Mn²⁺ excited state (⁴T₁) to Mn²⁺ ground state (⁶A₁). The emission wavelength implies that Mn²⁺ ions are

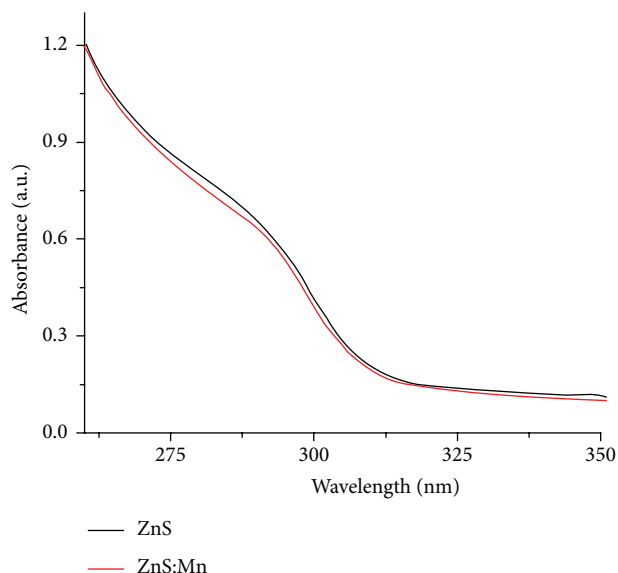


FIGURE 3: UV-visible spectra of ZnS QDs (black) and ZnS:Mn²⁺ QDs (red).

partly doped inside the nanocrystal volume and part of residue stay on the surface. Intrinsic PL emission in undoped ZnS QDs peaking around 400 nm (due to the vacancy of S²⁻ ions in undoped ZnS QDs) was not quenched in ZnS:Mn²⁺ QDs. After doping Mn²⁺, the fluorescence intensity increased severely and the intensity around 585 nm of ZnS:Mn²⁺ QDs magnifies 2 times compared to undoped ZnS QDs. Undoped and Mn²⁺-doped ZnS quantum dots were synthesized under exactly the same experimental conditions (aside from the presence of Mn). This result shows that there is a strong interaction between the d-electron states of Mn²⁺ ions and the s-p states of ZnS host lattice, providing an effective channel for the transfer of electrons and holes leading to the subsequent emission in ZnS:Mn²⁺ QDs.

The measured UV-visible absorption spectrum shows resolvable one-photon absorption induced optical transitions from valence subbands to conduction subbands of ZnS and ZnS:Mn²⁺ QDs, depicted in Figure 3, with a wide absorption peak from 325 nm to 285 nm, showing the first excitonic transition from S_{3/2}(h) to 1S(e) and the second excitonic transition from 2S_{3/2}(h) to 1S(e) at 325 nm (3.9 eV) and 285 nm (4.24 eV), respectively. Compared with ZnS QDs, after doping Mn²⁺, the absorbance of ZnS:Mn²⁺ QDs emerged to a small blue shift. However, except for the blue shift in the band edge, no other interesting phenomenon was observed. As expected, the amount of Mn²⁺ ions that can be incorporated in smaller-size ZnS quantum dots is lower. Moreover, the subtle but consistent blue shift in the optical absorption feature of ZnS:Mn²⁺ QDs reveals the formation of a smaller particle size because of the presence of the Mn-related additive.

3.2. Optimization of Experimental Conditions. The introduction of impurity ions into the host lattice can significantly

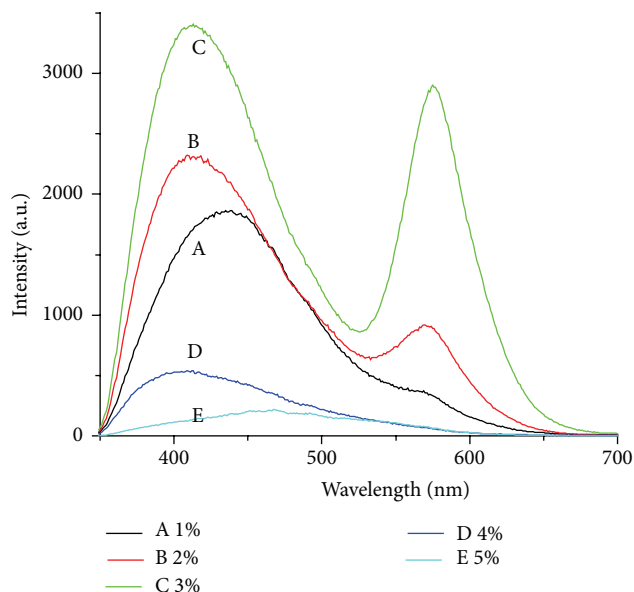


FIGURE 4: Fluorescence emission spectra of ZnS:Mn²⁺ QDs under the different doping level of Mn (from 1.0% to 5.0%). The excitation wavelength for all the samples was fixed at 300 nm.

depend on the reaction parameters, so the Mn precursor concentration, the pH of an aqueous solution, the reaction temperatures, and reaction times were investigated in this literature.

Band-edge luminescence and Mn²⁺-related luminescence are competing processes. The absorption of a photon leads to the formation of an exciton. The Mn precursor concentration in the reaction solutions was varied from 1.0% to 5.0%. Nevertheless, an increase in the Mn²⁺ concentration in the precursor solution above 5.0% caused significant deterioration in the luminescence, perhaps because of multiphase formation in the quantum dots (leading to defect states, which quench the luminescence). In this report, we mainly discuss ZnS:Mn²⁺ QDs formed with amounts of Mn in the solution less than or equal to 5.0%. As shown in Figure 4, Mn²⁺ doping clearly leads to near-band-edge luminescence at 413 nm and the ⁴T₁(4G) f⁶A₁(6S) manganese orange emission band at about 585 nm for 3.0% Mn²⁺ in ZnS quantum dots. Moreover, an increase in Mn²⁺ from 1.0% to 3.0% in the ZnS quantum dots causes a subtle red shift (by about 24 nm) in the wavelength of the orange luminescence and a blue shift in the near-band-edge luminescence wavelength (by about 22 nm). An increase in the doping level (from 1.0% to 3.0%) obviously leads to the increase in the intensity of the Mn²⁺-related ⁴T₁(4G) f⁶A₁(6S) transition. The Mn²⁺-related d-d transition is forbidden on the basis of dipole transition rules, but the Mn²⁺-related d-d transition opens up because of crystal field effects on the lattice. The very appearance of the distinct feature around 585 nm and the further enhancement in the intensity of the orange luminescence with increasing Mn²⁺ doping concentration are a signature of the incorporation of Mn²⁺ into the ZnS quantum dots. However, after the content of Mn²⁺ increases to 3.0%, the decrease in the energy

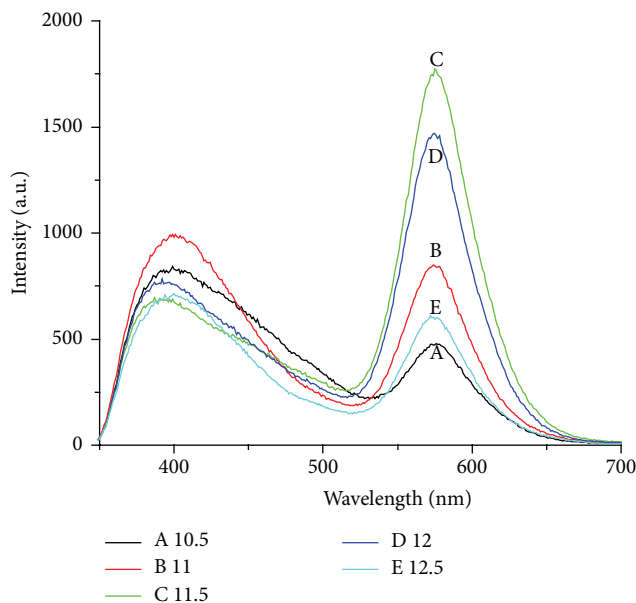


FIGURE 5: Fluorescence emission spectra of ZnS:Mn²⁺ QDs under the different pH value of an aqueous solution (from 10.5 to 12.5), obtained using an excitation wavelength of 300 nm.

of orange emission is caused by enhanced Mn-Mn interactions. Thus, 3.0% is chosen for ZnS:Mn²⁺ QDs synthesis.

The synthesis of ZnS:Mn²⁺ QDs is dependent on the pH of an aqueous solution; L-cysteine can resolve to ⁻SCH₂CH(NH₂)COO⁻ complexation with Zn²⁺ and Mn²⁺ easily in alkaline condition, which is apt to prepare ZnS:Mn²⁺ QDs. As shown in Figure 5, an increase in the pH of an aqueous solution (from 10.5 to 11.5) obviously leads to the increase in the fluorescence intensity of ZnS:Mn²⁺ QDs, upon pH of up to 11.5, the emission intensities of the samples to be maximized, and then decreases a little with higher pH. This fact makes us infer that zinc ion exists in solution with Zn(OH)₂ and Zn(OH)₄²⁻ while the pH is up to 11.5, which is apt to react with ⁻SCH₂CH(NH₂)COO⁻ and form ZnS:Mn²⁺ QDs successfully. Thus, the pH of an aqueous solution at 11.5 is chosen for ZnS:Mn²⁺ QDs synthesis.

The reaction temperature is one of key factors to influence the size and shape of ZnS:Mn²⁺ QDs and affect high quantum efficiency consequently. When the ZnS:Mn²⁺ QDs were prepared using Mn(CH₃COO)₂·4H₂O as the source of Mn and different reaction temperatures, a significant change in fluorescence intensity was observed (Figure 6). As shown in Figure 6, while the reaction temperature at 30°C, the Mn²⁺ orange luminescence exhibited at 565 nm and the band-edge luminescence exhibited at 413 nm with weak peaks, for a 3.0% doping level of Mn²⁺ in the ZnS quantum dots. Compared with ZnS:Mn²⁺ QDs were prepared at 30°C, ZnS:Mn²⁺ QDs were prepared at 50°C causing a subtle blue shift from 565 nm to 585 nm in the wavelength of the orange luminescence and a red shift from 413 nm to 426 nm in the near-band-edge luminescence wavelength. Moreover, with the reaction temperature increasing (from 30°C to 50°C), the fluorescence

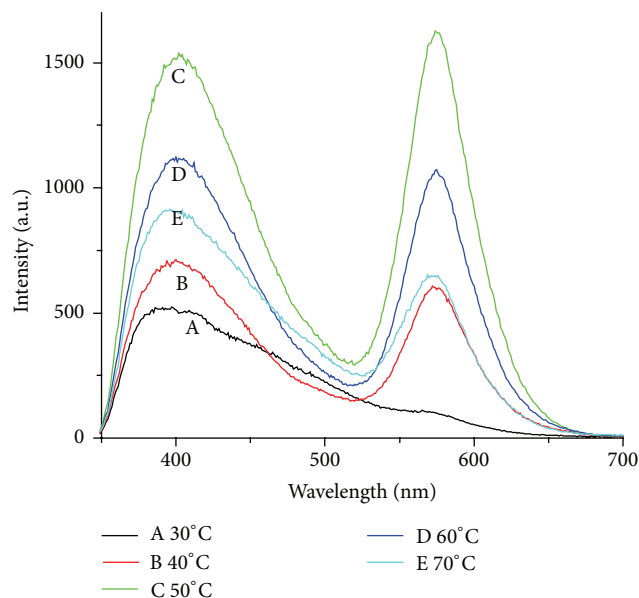


FIGURE 6: Fluorescence emission spectra of ZnS:Mn²⁺ QDs under the different reaction temperature (from 30°C to 70°C), obtained using an excitation wavelength of 300 nm.

intensity of ZnS:Mn²⁺ QDs increases sharply, the emission intensities of the samples to be maximized at 50°C, and then decreases a little with higher temperature. Thus, 50°C is chosen for ZnS:Mn²⁺ QDs synthesis.

PL spectra were recorded at the reaction times ranging from 3 h to 5.5 h (Figure 7). As the reaction times increased from 3 h to 4.5 h, the band-edge luminescence was red shifted from 401 to 413 nm, whereas the Mn²⁺ orange luminescence exhibited a blue shift from 585 to 582 nm. For all other concentrations, a similar effect was observed. An increase in the reaction times (from 3 h to 4.5 h) obviously leads to the increase in the fluorescence intensity of ZnS:Mn²⁺ QDs, the emission intensities of the samples to be maximized at 4.5 h, and then the emission intensities decreases sharply in higher reaction times (at 5 h and 5.5 h). Thus, 4.5 h is chosen for the optimal reaction time of ZnS:Mn²⁺ QDs synthesis.

In conclusion, the optimal reaction conditions of ZnS:Mn²⁺ QDs were obtained as follows: the doping level of Mn²⁺ is 3.0%, the pH of solution is 11.5, the reaction temperature is 50°C, and reaction time is 4.5 h. ZnS:Mn²⁺ QDs were prepared under such optimal reaction conditions having high quality of photophysical properties and narrow size distribution.

3.3. Absorption Characteristics of the HA-ZnS:Mn²⁺ QDs System. It has been shown that HA is not only an effective phototherapeutic agent but also a good photosensitizer [22]. Although the photochemical and photophysical properties of HA have been reported [23, 24], photosensitization of semiconductor with HA is little reported. Absorption spectra and fluorescence quenching afforded useful information concerning the process of electron injection from singlet excited state of HA to the conduction band of ZnS:Mn²⁺

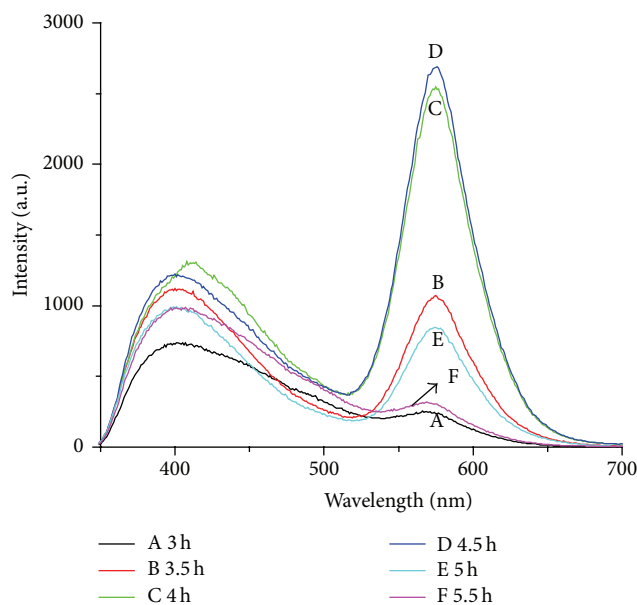


FIGURE 7: Fluorescence emission spectra of ZnS:Mn²⁺ QDs under different reaction times (from 3 h to 5.5 h), obtained using an excitation wavelength of 300 nm.

QDs. In this literature, electron transfer between HA and ZnS:Mn²⁺ QDs has been studied through absorption spectra and fluorescence quenching.

Absorption spectra of HA (A), ZnS:Mn²⁺ QDs (B), and HA-ZnS:Mn²⁺ QDs system (C) are shown in Figure 8. HA shows four peaks at around 280 nm, 485 nm, 540 nm, and 586 nm in Figure 8(b); note that the observation is in good similarity with that reported literature [25]. The ZnS:Mn²⁺ QDs have two peaks: the lowest peak is present around 325 nm and the second lowest peak is present around 285 nm (Figure 8(B)). As shown in Figure 8(C), the increases in the extinction coefficient and the red shift of the absorption maxima in the absorption spectra of HA in the presence of ZnS:Mn²⁺ QDs demonstrate the occurrence of surface interactions between the sensitizer and the particle surface. The irreversible nature of the decrease of absorbance of the HA on the ZnS:Mn²⁺ QDs is consistent with dye degradation [26].

The present study employed HA as sensitizer to investigate the adsorption details on the surface of the ZnS:Mn²⁺ QDs and the mechanism of the interfacial electron-transfer process from singlet state of HA to conduction band of ZnS:Mn²⁺ QDs in aqueous solution. In an aqueous solution, the colloidal ZnS:Mn²⁺ QDs can be assumed to have predominantly Zn-OH groups at the surface of ZnS:Mn²⁺ QDs, through which polar species in solution can strongly interact with the particles; HA can associate with ZnS:Mn²⁺ QDs through its polar groups such as OH and/or C=O, and this association will lead to a change of the p-electron distribution in HA molecule. As a result, as shown in Figure 9, an increase in the molar absorptivity and extended absorption of HA into the visible region were observed as the concentration of ZnS:Mn²⁺ QDs was increased. This made HA bound to

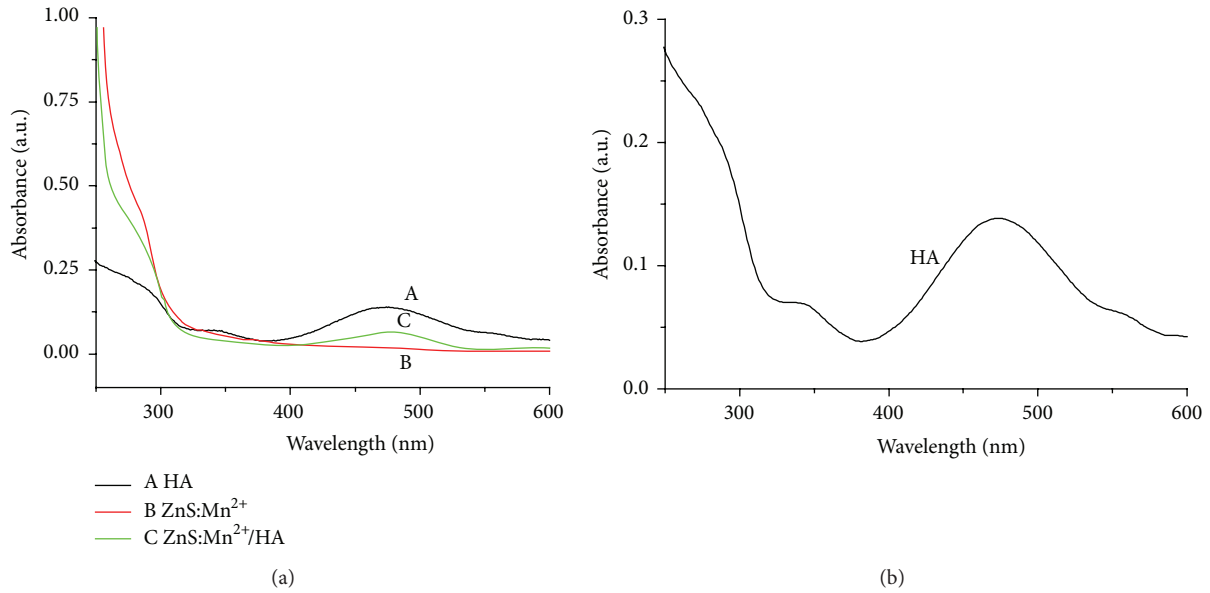


FIGURE 8: (a) Absorption spectra of HA (A), ZnS:Mn²⁺ QDs (B), and HA-ZnS:Mn²⁺ QDs system (C); (b) an image of absorption spectra of HA.

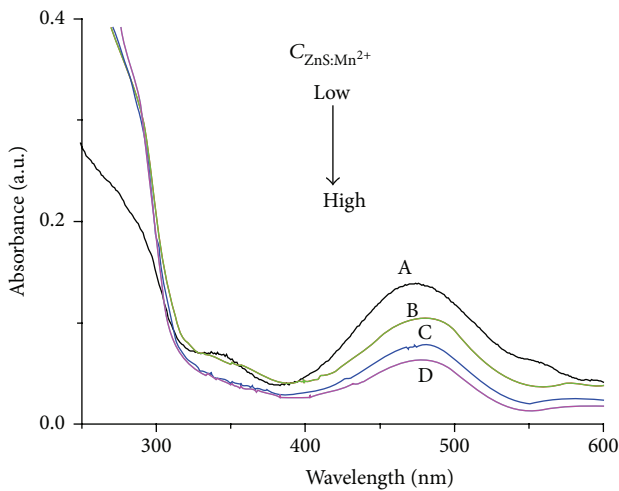


FIGURE 9: Absorption spectra of HA-ZnS:Mn²⁺ QDs system. The HA concentration was fixed at 1.8315×10^{-4} M and the concentration of ZnS:Mn²⁺ QDs (8.0143×10^{-3} M) increased from top to bottom.

ZnS:Mn²⁺ QDs as a good candidate for the purpose of photosensitization.

3.4. Fluorescence Quenching by ZnS:Mn²⁺ QDs. The fluorescence emission of HA was quenched upon successive addition of ZnS:Mn²⁺ QDs to a solution of 1.8315×10^{-4} M HA (Figure 10). This quenching behavior was similar to that of other organic dyes used for the sensitization of large-band gap semiconductors [25], which were caused by the electron injection from the singlet excited state of sensitizers to the conduction band of colloidal ZnS:Mn²⁺ QDs. This suggested that there was a complex association between HA and

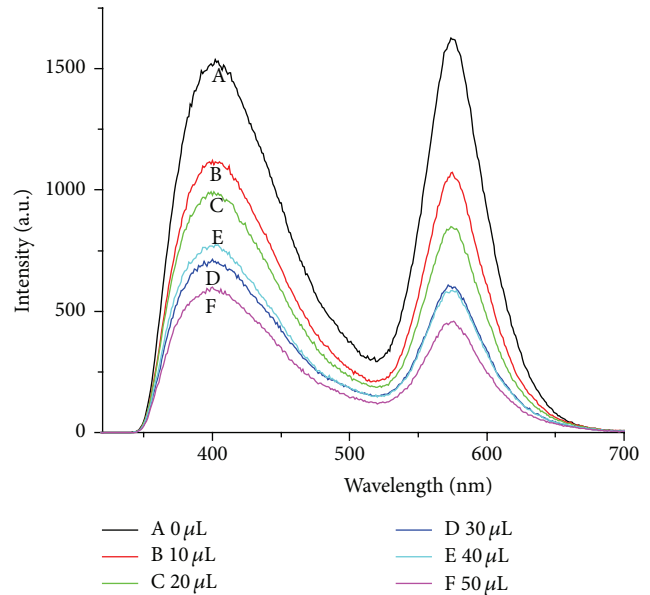


FIGURE 10: Fluorescence emission spectra of HA-ZnS:Mn²⁺ QDs system. The HA concentration was fixed at 1.8315×10^{-4} M and the concentration of ZnS:Mn²⁺ QDs (8.0143×10^{-3} M) increased from 0 μ L to 50 μ L, obtained using an excitation wavelength of 300 nm.

ZnS:Mn²⁺ QDs, which was necessary for observing the heterogeneous electron-transfer process at the interface of sensitizer-semiconductor.

4. Conclusions

Following growth doping technique, highly luminescent Mn-doped ZnS nanocrystals were synthesized and revealed

remarkably intense photoluminescence with the ${}^4T_1(4G)$ $f^6A_1(6S)$ transition in this literature. The dopant emission has been optimized with varying reaction parameters and found the optimal doping level of Mn. The method is simple, is hassle-free, and can be prepared to the high quality of Mn-doped ZnS nanocrystals. Photoluminescence (PL) emission measurements of ZnS:Mn $^{2+}$ QDs show Mn $^{2+}$ -related orange luminescence. Moreover, the electron transfer from singlet states of hypocrellin A (HA) to colloidal ZnS:Mn $^{2+}$ QDs has been examined by absorption and fluorescence quenching. The absorption spectrum gave an evidence of the strong association between HA and ZnS:Mn $^{2+}$ QDs; the electron could be injected from singlet excited states of HA to conduction band of colloidal ZnS:Mn $^{2+}$ QDs. PL measurements also suggested that there was a complex association between HA and ZnS:Mn $^{2+}$ QDs.

Conflict of Interests

The authors declare that there is no conflict of interests regarding the publication of this paper.

Acknowledgments

The authors gratefully acknowledge the financial support from the National Science Foundation of China (61361002 and 21362010) and Yunnan Provincial Department of Education General Project (2013Y067).

References

- [1] R. Subha, V. Nalla, J. H. Yu et al., "Efficient photoluminescence of Mn $^{2+}$ -doped ZnS quantum dots excited by two-photon absorption in near-infrared window II," *Journal of Physical Chemistry C*, vol. 117, no. 40, pp. 20905–20911, 2013.
- [2] W. Zhang, Y. Li, H. Zhang, X. Zhou, and X. Zhong, "Facile synthesis of highly luminescent Mn-doped ZnS nanocrystals," *Inorganic Chemistry*, vol. 50, no. 20, pp. 10432–10438, 2011.
- [3] Y. B. Wang, X. H. Liang, X. Ma et al., "Simple and greener synthesis of highly photoluminescence Mn $^{2+}$ -doped ZnS quantum dots and its surface passivation mechanism," *Applied Surface Science*, vol. 316, pp. 54–61, 2014.
- [4] O. Kolmykov, J. Coulon, J. Lalevée, H. Alem, G. Medjahdi, and R. Schneider, "Aqueous synthesis of highly luminescent glutathione-capped Mn $^{2+}$ -doped ZnS quantum dots," *Materials Science and Engineering C*, vol. 44, pp. 17–23, 2014.
- [5] M. Stefan, S. V. Nistor, and D. Ghica, "Correlation of lattice disorder with crystallite size and the growth kinetics of Mn $^{2+}$ -doped ZnO nanocrystals probed by electron paramagnetic resonance," *Crystal Growth & Design*, vol. 13, no. 3, pp. 1350–1359, 2013.
- [6] R. Begum, S. Bhandari, and A. Chattopadhyay, "Surface ion engineering of Mn $^{2+}$ -doped ZnS quantum dots using ion-exchange resins," *Langmuir*, vol. 28, no. 25, pp. 9722–9728, 2012.
- [7] H. Li, W. Y. Shih, and W.-H. Shih, "Highly photoluminescent and stable aqueous ZnS quantum dots," *Industrial & Engineering Chemistry Research*, vol. 49, no. 2, pp. 578–582, 2010.
- [8] V. K. Chandra, B. P. Chandra, and P. Jha, "Mechanoluminescence of ZnS: Mn phosphors excited by hydrostatic pressure steps and pressure pulses," *Physica B: Condensed Matter*, vol. 452, pp. 23–30, 2014.
- [9] R. Begum and A. Chattopadhyay, "In situ reversible tuning of photoluminescence of Mn $^{2+}$ -doped ZnS quantum dots by redox chemistry," *Langmuir*, vol. 27, no. 10, pp. 6433–6439, 2011.
- [10] H. Wu and Z. Fan, "Mn-doped ZnS quantum dots for the room-temperature phosphorescence detection of raceniso-damine hydrochloride and atropine sulfate in biological fluids," *Spectrochimica Acta Part A: Molecular and Biomolecular Spectroscopy*, vol. 90, pp. 131–134, 2012.
- [11] M. B. Xu, T. Ye, S. Y. Lu, Q. Q. Hu, J. Zhou, and J. Q. Lu, "Synthesis of bovine serum albumin imprinted Mn:ZnS quantum dots," *Chinese Chemical Letters*, vol. 23, no. 12, pp. 1403–1406, 2012.
- [12] S. N. Azizi, P. Shakeri, M. J. Chaichi, A. Bekhradnia, M. Taghavi, and M. Ghaemy, "The use of imidazolium ionic liquid/copper complex as novel and green catalyst for chemiluminescent detection of folic acid by Mn-doped ZnS nanocrystals," *Spectrochimica Acta Part A: Molecular and Biomolecular Spectroscopy*, vol. 122, pp. 482–488, 2014.
- [13] A. Goudarzi, G. M. Aval, S. S. Park et al., "Low-temperature growth of nanocrystalline Mn-doped ZnS thin films prepared by chemical bath deposition and optical properties," *Chemistry of Materials*, vol. 21, no. 12, pp. 2375–2385, 2009.
- [14] G. R. Patzke, F. Krumeich, and R. Nesper, "Oxidic nanotubes and nanorods—anisotropic modules for a future nanotechnology," *Angewandte Chemie International Edition*, vol. 41, no. 14, pp. 2446–2461, 2002.
- [15] Y. Tian, Y. Z. Zhao, H. Q. Tang, W. W. Zhou, L. G. Wang, and J. Zhang, "Synthesis of ZnS ultrathin nanowires and photoluminescence with Mn $^{2+}$ doping," *Materials Letters*, vol. 148, pp. 151–154, 2015.
- [16] H. Li, X. Wang, J. Xu et al., "One-dimensional CdS nanostructures: a promising candidate for optoelectronics," *Advanced Materials*, vol. 25, no. 22, pp. 3017–3037, 2013.
- [17] P. A. G. Beermann, B. R. McGarvey, S. Muralidharan, and R. C. W. Sung, "EPR spectra of Mn $^{2+}$ -doped ZnS quantum dots," *Chemistry of Materials*, vol. 16, no. 5, pp. 915–918, 2004.
- [18] B. B. Srivastava, S. Jana, N. S. Karan et al., "Highly luminescent Mn-doped ZnS nanocrystals: gram-scale synthesis," *The Journal of Physical Chemistry Letters*, vol. 1, no. 9, pp. 1454–1458, 2010.
- [19] W. Liu, X. L. Chen, L. S. Yang et al., "Photochemical events during the photosensitization of hypocrellin A on ZnS quantum dots," *Advanced Materials Research*, vol. 581–582, no. 1, pp. 574–577, 2012.
- [20] Y.-Y. He, H.-Y. Liu, J.-Y. An, R. Han, and L.-J. Jiang, "Photodynamic action of hypocrellin dyes: structure-activity relationships," *Dyes and Pigments*, vol. 44, no. 1, pp. 63–67, 1999.
- [21] H. Brockman and D. Spitzner, "D. K. d. Pseudohypericins," *Chemische Berichte*, vol. 37, p. 108, 1975.
- [22] J. N. Ma, L. J. Jiang, M. H. Zhang, and Q. Yu, "Delayed fluorescence of hypocrellins and absorption spectra of isomers," *Chinese Science Bulletin*, vol. 34, pp. 1442–1448, 1989.
- [23] Z. J. Diwu and J. W. Lown, "Photosensitization by anticancer agents 12. Perylene quinonoid pigments, a novel type of singlet oxygen sensitizer," *Journal of Photochemistry and Photobiology A: Chemistry*, vol. 64, no. 3, pp. 273–287, 1992.
- [24] Z. J. Diwu and J. W. Lown, "Photosensitization with anticancer agents 14. Perylenequinonoid pigments as new potential photodynamic therapeutic agents: formation of tautomeric semiquinone radicals," *Journal of Photochemistry and Photobiology A: Chemistry*, vol. 69, no. 2, pp. 191–199, 1992.

- [25] J. Moser and M. Gratzel, "Photosensitized electron injection in colloidal semiconductors," *Journal of the American Chemical Society*, vol. 106, no. 22, pp. 6557–6564, 1984.
- [26] M. Zhou, X. F. Chen, Y. Y. Xu et al., "Sensitive determination of Sudan dyes in foodstuffs by Mn–ZnS quantum dots," *Dyes and Pigments*, vol. 99, no. 1, pp. 120–126, 2013.



Hindawi

Submit your manuscripts at
<http://www.hindawi.com>

